THE BELL SYSTEM TECHNICAL JOURNAL
Vol. 52, No. 6, July–August, 1973
Printed in U.S.A.

On the Selection of a Two-Dimensional Signal Constellation in the Presence of Phase Jitter and Gaussian Noise

By G. J. FOSCHINI, R. D. GITLIN, and S. B. WEINSTEIN

(Manuscript received February 1, 1973)

A long-standing communications problem is the efficient coding of a block of binary data into a pair of in-phase and quadrature components. This modulation technique may be regarded as the placing of a discrete number of signal points in two dimensions. Quadrature amplitude modulation (QAM) and combined amplitude and phase modulation (AM-PM) are two familiar examples of this signaling format. Subject to a peak or average power constraint, the selection of the signal coordinates is done so as to minimize the probability of error. In the design of high-speed data communication systems this problem becomes one of great practical significance since the dense packing of signal points reduces the margin against Gaussian noise. Phase jitter, which tends to perturb the angular location of the transmitted signal point, further degrades the error rate. Previous investigations have considered the signal evaluation and design problem in the presence of Gaussian noise alone and within the framework of a particular structure, such as conventional amplitude and phase modulation. We present techniques to evaluate and optimize the choice of a signal constellation in the presence of both Gaussian noise and carrier phase jitter. The performance of a number of currently used or proposed signal constellations are compared.

The evaluation and the optimization are based upon a perturbation analysis of the probability density of the received signal given the transmitted signal. Laplace's asymptotic formula is used for the evaluation. Discretizing the signal space reduces the optimal signal design problem under a peak power constraint to a tractable mathematical programming problem.

Our results indicate that in Gaussian noise alone an improvement in signal-to-noise ratio of as much as 2 dB may be realized by using quadrature amplitude modulation instead of conventional amplitude and phase

modulation. New modulation formats are proposed which perform very well in Gaussian noise and additionally are quite insensitive to moderate amounts of phase jitter.

I. INTRODUCTION

A very attractive modulation format for coherent high-speed data transmission is the family of suppressed-carrier, two-dimensional signal constellations of which quadrature amplitude modulation (QAM) and combined amplitude and phase modulation (AM-PM) are two examples. In this paper we will consider using this more general signal format, which is equivalent to the arbitrary placement of a discrete number of signal points in the plane, subject only to a peak or average power constraint. The object will be to mitigate the major *statistical* transmission impairments encountered on the voice-grade telephone channel, such as carrier frequency offset, carrier phase jitter, and additive noise. Our attention is focused on constellations of 16 points, since this seems to be the largest constellation which is practical for the typical telephone channel. However, the techniques we develop are applicable to constellations of arbitrary size.

The placing of signal points in the plane is a long-standing problem that has received considerable attention in the past. Previous investigations[1–3] have considered the signal evaluation and design problem in the presence of Gaussian noise alone and within the framework of a particular structure such as combined amplitude and phase modulation. When Gaussian noise is the only transmission impairment, it is well known that at high signal-to-noise ratios (>25 dB) the signal points should be placed as far apart from each other as possible (the circle-packing problem). In the application to high-speed digital communication systems, the two-dimensional signal design problem becomes one of great practical significance because the dense packing of a large number of signal points markedly reduces the margin against random noise and phase jitter. The signal design problem in the presence of both phase jitter and Gaussian noise has not been solved before and is the subject of our discussion.

Coherent receiver structures have recently been proposed which employ an adaptive equalizer[4] to compensate for any linear distortion, low-frequency phase jitter, or small amounts of frequency offset introduced by the channel. A phase-locked loop[5] may be used to suppress high-frequency phase jitter and frequency offset. Of course, the output of a phase-locked loop will still deviate somewhat from the optimum demodulating phase angle. One purpose of this study is to assess the

effect of such phase errors on the system error rate and to indicate how this knowledge can be incorporated into the system design.

By system design we have in mind the selection of both a particular two-dimensional signaling format and the decision device placed at the demodulator output. In order to pursue these objectives, we discuss:

(*i*) the relative immunity of various signal constellations as a function of the degree of noncoherency (i.e., the size of the phase error);
(*ii*) an efficient iterative procedure for determining optimum signal formats under a peak power constraint;
(*iii*) system performance for the following hierarchy of decision devices: easily implementable, optimum in Gaussian noise, and a maximum-likelihood detector which uses the statistics of the phase error;
(*iv*) the accuracy required in any phase-locked loop to attain a satisfactory error rate; and
(*v*) the resulting error rate when no attempt is made to track the jitter.*

Our approach is to assume that intersymbol interference has been effectively eliminated by the equalizer while the phase-locked loop, if there is one, has only partially removed the phase jitter. Thus the equalizer output will be the sum of the partially coherent† transmitted signal and additive Gaussian noise. We adopt a phenomenological model which assumes that the (slowly varying) phase error has a Tikhonov density.[5] The Tikhonov density is associated with a conventional first-order phase-locked loop whose input is the sum of a sinusoid (whose phase is being tracked by the loop) and Gaussian noise. Under our assumed operating conditions of high signal-to-noise ratio, this density will closely approximate the actual phase density. When no attempt at tracking is made,‡ the jitter is modeled as being uniformly distributed in a reasonable peak-to-peak range. For each of these jitter densities, the probability density of the demodulator output, conditioned on the transmitted symbol, is used to estimate the error rate. This estimate is of the minimum distance type, where the "distance," which reflects the presence of phase jitter, is measured in

* In the sequel, we will use the term jitter as a catch-all when referring to phase jitter and/or frequency offset.

† A partially coherent signal is one whose carrier phase is jittered by a random component which is *not* uniformly distributed in the range $(-\pi, \pi)$.

‡ Since the passband equalizer[4] will determine the optimum static demodulating phase, the absence of a phase-locked loop does not imply the use of an arbitrary demodulating phase.

a non-Euclidean manner. The error rate is given for various signal constellations and detector structures under peak and average power constraints. By discretizing the received signal space, an iterative procedure is developed to determine (locally) optimum signal formats under a peak power constraint. This technique, which assumes a maximum-likelihood detector, makes use of an efficient search procedure developed by Kernighan and Lin.[6]

The system model and the problem formulation are presented in Section II. An asymptotic estimate and an upper bound on the error rate are developed in Section III. A comparison of the relative immunity of some popular signal constellations and detectors to phase jitter is described in Section IV. Section V discusses a technique to obtain locally optimum signal structures under a peak power constraint.*

II. SYSTEM MODEL AND PROBLEM FORMULATION

2.1 *Preliminaries*

We consider the two-dimensional synchronous data communication system shown in Fig. 1. Binary data are first grouped into blocks of M bits, and each block of M bits is then mapped into one of 2^M two-tuples (a, b). The sequences $\{a_k\}$ and $\{b_k\}$ amplitude modulate, respectively, an in-phase and quadrature carrier to generate the transmitted signal

$$m(t) = \sum_k a_k p(t - kT) \cos \omega_c t + \sum_k b_k p(t - kT) \sin \omega_c t, \qquad (1)$$

where $1/T$ is the symbol rate,† $p(\cdot)$ represents the transmitter pulse shaping, and ω_c is the carrier frequency. It will be assumed that the two-tuples are equiprobable. The received signal at the output of the bandpass filter is given by

$$\begin{aligned} r(t) = {} & \Big(\sum_k a_k x(t - kT) - \sum_k b_k y(t - kT)\Big) \cos\left((\omega_c + \Delta)t + \theta(t)\right) \\ & - \Big(\sum_k a_k y(t - kT) + \sum_k b_k (t - kT)\Big) \\ & \times \sin\left((\omega_c + \Delta)t + \theta(t)\right) + n(t), \qquad (2) \end{aligned}$$

where $x(t)$ and $y(t)$ are the system (baseband) in-phase and quadrature impulse responses,‡ Δ is the carrier frequency offset, $\theta(t)$ is the random

* The present authors have recently treated the two-dimensional signal design problem under an average power constraint.[7]

† Note that the data rate is M/T bits/second.

‡ These pulses represent the cascade of the transmitter shaping filter, the channel, and the receiving filter.

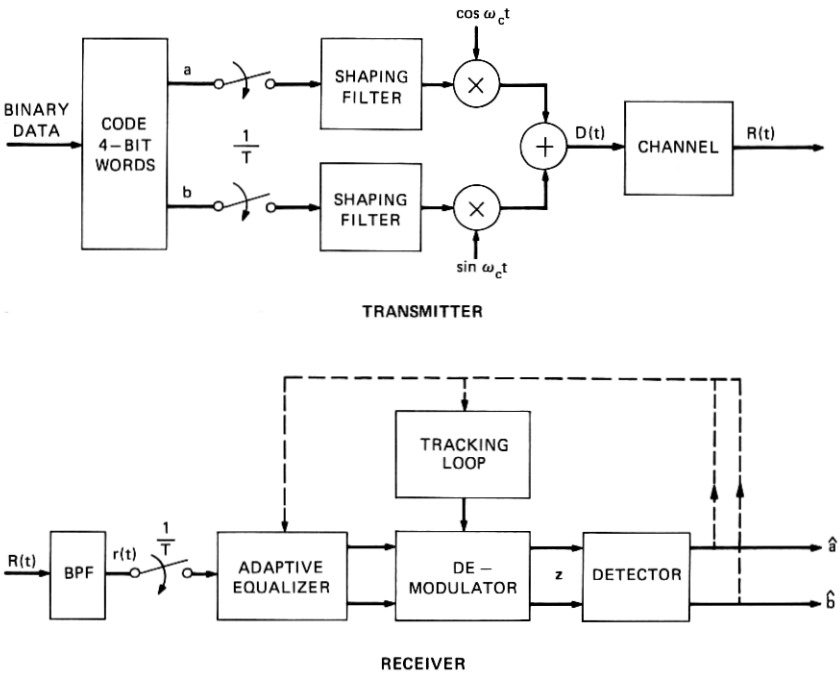

Fig. 1—An in-phase and quadrature data transmission system.

phase jitter, and $n(t)$ is additive Gaussian noise. The received signal, which is sampled at the symbol rate, is adaptively equalized and then coherently demodulated with the aid of a phase-locked loop.[5] The demodulated output, denoted by the sequence of two-tuples $\mathbf{z}_k = \{(z_k, \check{z}_k)\}$, is then processed by the (simple) detector to give the output sequence $\{(\hat{a}_k, \hat{b}_k)\}$. The system error rate is just the probability that $(\hat{a}_k, \hat{b}_k)$ differs from the transmitted two-tuple (a_k, b_k).

2.2 *Basic Model*

For the purposes of this study, it will be convenient to assume that the equalizer has completely eliminated the intersymbol interference present in $x(t)$ and $y(t)$, but that the phase-locked loop has only partially compensated for the carrier phase jitter. The in-phase and quadrature demodulator outputs, at the kth sampling instant, are then given by

$$\begin{aligned} z(kT) &= a_k \cos \phi_k - b_k \sin \phi_k + n_c(kT), \\ \check{z}(kT) &= a_k \sin \phi_k + b_k \cos \phi_k + n_s(kT), \end{aligned} \tag{3}$$

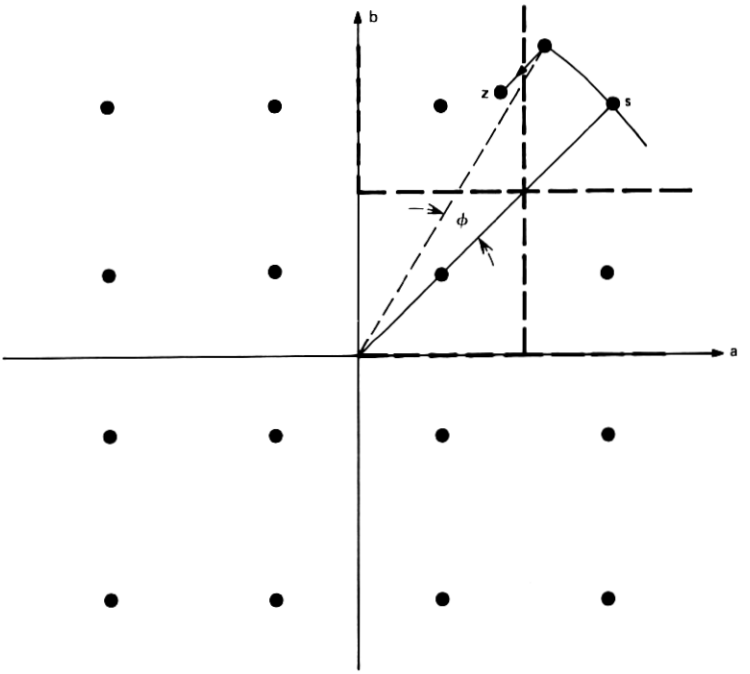

Fig. 2—Effect of Gaussian noise and phase jitter on transmitted symbol.

where ϕ_k is the (slowly varying) phase error in the tracking loop, and $n_c(kT)$ and $n_s(kT)$ are, respectively, the in-phase and quadrature Gaussian noise components.* Dropping the time index, eq. (3) can be rewritten to give the basic model

$$\mathbf{z} = R\mathbf{s} + \mathbf{n}, \tag{4}$$

where the vectors are given by†

$$\mathbf{z} = \begin{pmatrix} z \\ \check{z} \end{pmatrix}, \qquad \mathbf{s} = \begin{pmatrix} a \\ b \end{pmatrix}, \qquad \mathbf{n} = \begin{pmatrix} n_c \\ n_s \end{pmatrix},$$

and the matrix R is the rotational (by an angle ϕ) transformation

$$R = \begin{pmatrix} \cos\phi & -\sin\phi \\ \sin\phi & \cos\phi \end{pmatrix}. \tag{5}$$

* Recall that $n_c(kT)$ and $n_s(kT)$ are independent Gaussian random variables with equal variance, N_0. It should be noted that $2N_0$ is the noise power contained in the bandwidth of the received signal.

† We denote the values that a and b can assume by $a^{(j)}$ and $b^{(j)}$, respectively, and the values of the transmitted symbols by $\mathbf{s}^{(j)} = (a^{(j)}, b^{(j)})$.

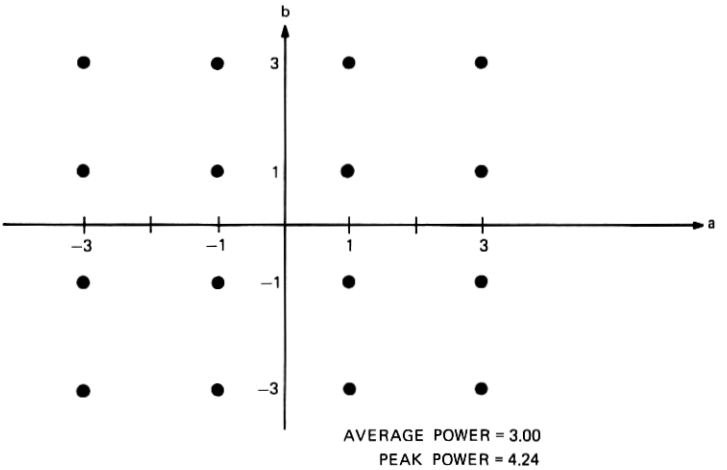

Fig. 3—Quadrature amplitude modulation.

As we show in Fig. 2, the effect of the phase jitter is to rotate the transmitted symbol, $\mathbf{s}$, by an angle ϕ; thus the demodulator output, $\mathbf{z}$, is dispersed in an angular manner due to phase jitter and in a circularly symmetric way due to the Gaussian noise. The receiver will make an error when these perturbations move the demodulator output across the decision boundary associated with the transmitted symbol. For a particular transmitted data sequence, the demodulated sequence will be scattered about the transmitted points in a manner which reflects the combined effects of phase jitter and Gaussian noise. For the transmitted signal constellation of Fig. 3, which is known as QAM, a typical scattered demodulated sequence is shown in Fig. 4. As one might expect, for those signal points further away from the origin, the angular displacement becomes more apparent. An estimate of this effect is given by the mean-square error between the transmitted and demodulated symbols. For small values of jitter, this error is obtained from (4) by noting that

$$\mathbf{z} - \mathbf{s}^{(j)} = \begin{pmatrix} \cos\phi - 1 & -\sin\phi \\ \sin\phi & \cos\phi - 1 \end{pmatrix} \mathbf{s}^{(j)} + \mathbf{n} \approx \phi \begin{pmatrix} -b_j \\ a_j \end{pmatrix} + \mathbf{n};$$

averaging the norm-squared of both sides gives*

$$E\|\mathbf{z} - \mathbf{s}^{(j)}\|^2 = N_0 + \sigma_\phi^2 \|\mathbf{s}^{(j)}\|^2, \tag{6}$$

* The notation $\|\mathbf{z}\|$ denotes the Euclidean norm of $\mathbf{z}$; additionally the notation $\langle \mathbf{z}, \mathbf{s} \rangle$ will be used to denote the inner product of $\mathbf{z}$ and $\mathbf{s}$.

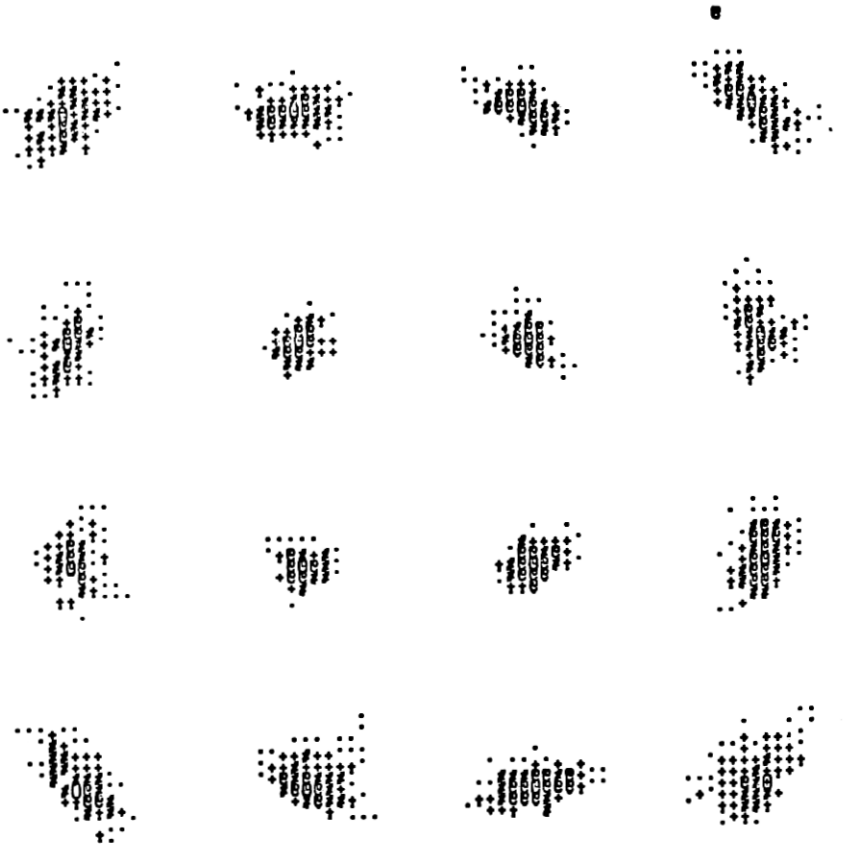

Fig. 4—Received signal points in a QAM system.

where σ_ϕ^2 is the variance of ϕ and E denotes the statistical average. Thus, because of phase jitter, signal points located further from the origin are subjected to a larger mean-square error.

2.3 *Probability Density of the Demodulator Output*

In order to evaluate the system error rate, the probability density function (pdf) of the phase error must be specified. The pdf of the phase error in a phase-locked loop that is tracking the angle of the two-dimensional data signal given by (2) is not yet known, but as explained below it can be approximated by the following (Tikhonov) density[5]:

$$p(\phi) = \frac{1}{2\pi} \frac{e^{\alpha \cos \phi}}{I_0(\alpha)}, \qquad |\phi| \leqq \pi, \tag{7}$$

where $I_0(\cdot)$ is the modified Bessel function of the first kind and α is a positive number. As is shown in Fig. 5, $\alpha = 0$ implies a completely incoherent system, while $\alpha = \infty$ corresponds to a completely coherent system. For large values of α ($\alpha > 100$), we have the useful relation

$$\sigma_\phi^2 \approx \frac{1}{\alpha} \qquad \text{(in radians)}. \tag{8}$$

Since the above density arises from a first-order phase-locked loop whose input is the sum of Gaussian noise and a sinusoid (whose phase is being tracked by the loop), it is felt that for high signal-to-noise ratio, for negligible intersymbol interference, and for slowly varying phase jitter the actual phase-error density will closely resemble the Tikhonov density. This simple model will be quite useful in studying the effect of phase jitter on the system error rate.

The pdf of the demodulator output, conditioned on the transmission of $\mathbf{s}^{(j)}$, is given by

$$p(\mathbf{z}\,|\,\mathbf{s}^{(j)}) \triangleq p_j(\mathbf{z}) = \int_{-\pi}^{\pi} p_j(\mathbf{z}\,|\,\phi)p(\phi)d\phi, \tag{9}$$

where it is noted that the output density conditioned on both $\mathbf{s}^{(j)}$ and ϕ is given by

$$p_j(\mathbf{z}\,|\,\phi) = \frac{1}{2\pi N_0} \exp\left[-\frac{1}{2N_0}\|\mathbf{z} - R\mathbf{s}^{(j)}\|^2\right] \tag{10a}$$

$$= \frac{1}{2\pi N_0} \exp\left\{-\frac{1}{2N_0}\left[\|\mathbf{z} - \mathbf{s}^{(j)}\|^2 + 2\langle \mathbf{z}, \mathbf{s}^{(j)}\rangle - 2\langle \mathbf{z}, R\mathbf{s}^{(j)}\rangle\right]\right\}. \tag{10b}$$

Substituting the Tikhonov density into (9) gives

$$p_j(\mathbf{z}) = \frac{1}{2\pi N_0} \exp\left\{-\frac{1}{2N_0}\left[\|\mathbf{z} - \mathbf{s}^{(j)}\|^2 + 2\langle \mathbf{z}, \mathbf{s}^{(j)}\rangle\right]\right\} \cdot (I_0(\alpha))^{-1} \frac{1}{2\pi} \int_{-\pi}^{\pi} \exp\frac{1}{N_0}\left[(\langle \mathbf{z}, \mathbf{s}^{(j)}\rangle + \alpha N_0)\cos\phi + \langle \mathbf{z}, \mathbf{s}^{(j)\perp}\rangle \sin\phi\right] d\phi, \tag{11}$$

(where if $\mathbf{s}^{(j)} = \|\mathbf{s}^{(j)}\|(\cos\alpha, \sin\alpha)$ then $\mathbf{s}^{(j)\perp} = \|\mathbf{s}^{(j)}\|(\sin\alpha, -\cos\alpha)$), and we recognize the latter integral as

$$I_0\left(\frac{1}{N_0}\sqrt{(\langle \mathbf{z}, \mathbf{s}^{(j)}\rangle + \alpha N_0)^2 + \langle \mathbf{z}, \mathbf{s}^{(j)\perp}\rangle^2}\right).$$

Assume $\alpha = k/N_0$ (k a constant). Employing the well-known result

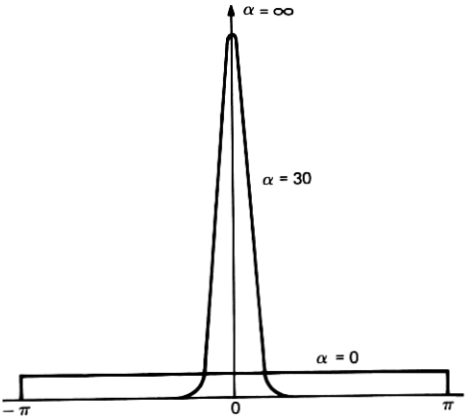

Fig. 5—Tikhonov phase jitter density $p(\phi) = \exp(\alpha \cos \phi)/2\pi I_0(\alpha)$.

that for large values of argument $I_0(x) \approx e^x/|\sqrt{x}|$, and assuming α is sufficiently large and N_0 is sufficiently small, we get

$$p_j(\mathbf{z}) \approx \frac{1}{2\pi N_0}\sqrt{\frac{\alpha N_0}{\sqrt{(\langle \mathbf{z}, \mathbf{s}^{(j)}\rangle + \alpha N_0)^2 + (\langle \mathbf{z}, \mathbf{s}^{(j)\perp}\rangle)^2}}} \exp\Bigg(-\frac{1}{2N_0} \times \{\|\mathbf{z}, \mathbf{s}^{(j)}\|^2 + 2\langle \mathbf{z}, \mathbf{s}^{(j)}\rangle + 2\alpha N_0 - 2\sqrt{(\langle \mathbf{z}, \mathbf{s}^{(j)}\rangle + \alpha N_0)^2 + \langle \mathbf{z}, \mathbf{s}^{(j)\perp}\rangle^2}\}\Bigg). \quad (12)$$

In the error rate computations we shall eventually make, we will have k so large compared to the practical range of $\langle \mathbf{z}, \mathbf{s}^{(j)}\rangle$ that the coefficient multiplying the exponential of $p_j(\mathbf{z})$ can be taken to be $(2\pi N_0)^{-1}$.

Thus, for our purposes,

$$p_j(\mathbf{z}) \approx \frac{1}{2\pi N_0} \exp\left[-\frac{1}{2N_0} d^2(\mathbf{z}, \mathbf{s}^{(j)})\right], \quad (13)$$

where

$$d^2(\mathbf{z}, \mathbf{s}) \triangleq \|\mathbf{z} - \mathbf{s}\|^2 + 2\langle \mathbf{z}, \mathbf{s}\rangle + 2\alpha N_0 - 2|\sqrt{\|\mathbf{z}\|^2\|\mathbf{s}\|^2 + 2\alpha N_0\langle \mathbf{z}, \mathbf{s}\rangle + (\alpha N_0)^2}|. \quad (14)$$

The form of eq. (13) is very reminiscent of the density in Gaussian noise alone, and to further suggest such a similarity we refer to $d(\mathbf{z}, \mathbf{s})$ as the "distance" between $\mathbf{z}$ and $\mathbf{s}$. It is important to emphasize that this function is the key to assessing the combined effect of Gaussian noise and phase jitter on the system performance; through its use we

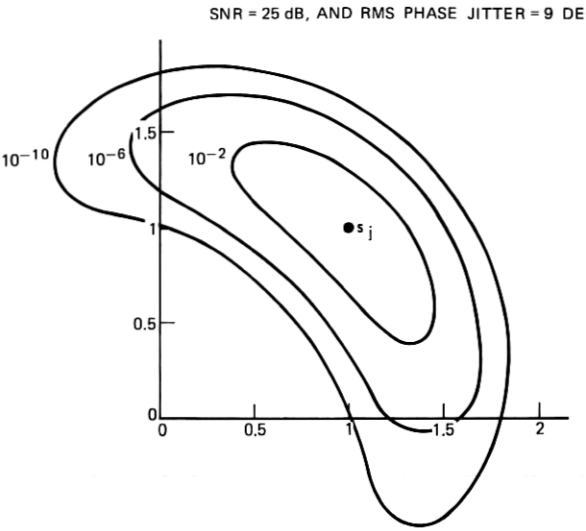

Fig. 6—Constant distance contours: values of $\mathbf{z}$ for which

$$2\pi N_0 p_j(\mathbf{z}) = \exp\left\{-\frac{1}{2N_0} d^2(\mathbf{z}, \mathbf{s}_j)\right\} = 10^{-2}, 10^{-6}, 10^{-10}.$$

d^2 given by eq. (14).

are able to give a very suggestive geometric interpretation of the jitter phenomenon as well as accurate estimates of the error rate. In Fig. 6 we show some contours of constant "distance" (i.e., points which are equiprobable) about a given point. Note the angular orientation and similarity of these "banana" shaped contours to those obtained experimentally (Fig. 4).

Our procedure will be to use (13) and (14) to estimate the error rate for various constellations and detector structures; however, before we do this, we first wish to discuss some properties of the function $d(\mathbf{z}, \mathbf{s})$ which will be useful in estimating the system performance, and then to consider the conditional density $p_j(\mathbf{z})$ in the absence of a phase-locked loop.

2.4 *Some Properties of the Jitter Distance* $d(\mathbf{z}, \mathbf{s})$

(*i*) A requisite property that $d(\mathbf{z}, \mathbf{s})$ should possess is that for vanishingly small jitter the distance between points becomes Euclidean. This is easily verified by expanding (14) in terms of $1/\alpha$ and observing that

$$\lim_{1/\alpha \to 0} d^2(\mathbf{z}, \mathbf{s}) = \|\mathbf{z} - \mathbf{s}\|^2. \tag{15}$$

(*ii*) Since we do not expect the distance between an arbitrary point and the origin to be affected by phase jitter, it is reassuring to note that

$$d^2(\mathbf{z}, \mathbf{0}) = \|\mathbf{z}\|^2, \tag{16}$$

and that a similar property holds for points on the same ray, i.e.,

$$d^2(\mathbf{z}, k\mathbf{z}) = (1 - k)^2\|\mathbf{z}\|^2, \qquad k > 0. \tag{17}$$

(*iii*) A "bonus" property is that even though (14) was derived for large α (small jitter), the expression

$$\lim_{\alpha \to 0} d^2(\mathbf{z}, \mathbf{s}) = | \, \|\mathbf{z}\| - \|\mathbf{s}\| \, |^2 \tag{18}$$

is quite reasonable in that, for completely incoherent systems, all points on the same circle are indistinguishable.

(*iv*) An interesting consequence of (14) is that points are now *closer* together than their Euclidean distance. To demonstrate this, we use the Schwartz inequality to show that the non-Euclidean part of $d^2(\mathbf{z}, \mathbf{s})$ is always negative, i.e.,

$$\langle \mathbf{z}, \mathbf{s} \rangle + \alpha N_0 \leqq |\sqrt{\|\mathbf{z}\|^2\|\mathbf{s}\|^2 + 2\alpha N_0\langle \mathbf{z}, \mathbf{s} \rangle + (\alpha N_0)^2}| \tag{19}$$

since squaring gives

$$\langle \mathbf{z}, \mathbf{s} \rangle^2 + 2\alpha N_0\langle \mathbf{z}, \mathbf{s} \rangle + (\alpha N_0)^2 \leqq \|\mathbf{z}\|^2\|\mathbf{s}\|^2 + 2\alpha N_0\langle \mathbf{z}, \mathbf{s} \rangle + (\alpha N_0)^2$$

which upon cancelling becomes the Schwartz inequality

$$\langle \mathbf{z}, \mathbf{s} \rangle^2 \leqq \|\mathbf{z}\|^2\|\mathbf{s}\|^2.$$

(*v*) If both the signal and noise power are scaled by the same constant for a given jitter level, α, it is clear that the conditional density is unchanged. Thus the signal-to-noise ratio and the mean-square jitter α are the natural parameters for characterizing the system.

(*vi*) A natural question to ask is whether or not $d(\mathbf{z}, \mathbf{s})$ is a convex metric* in the plane or, of more practical interest, if some sufficiently accurate approximation to $d(\mathbf{z}, \mathbf{s})$ is a convex metric in some circle centered about the origin. As we shall see later, if such an approximate representation can be obtained, some tedious error rate computations may be done quite simply. *While the requirements of symmetry and positivity can easily be shown to hold in the entire plane, J. E. Mazo has recently informed us that his results in Ref. 8 imply that* $d(\mathbf{z}, \mathbf{s})$ *is not a*

* A convex metric is a metric which possesses the midpoint property, i.e., for any two points $\mathbf{x}$ and $\mathbf{y}$ there is always a third point $\mathbf{z}$ such that $d(\mathbf{x}, \mathbf{z}) = d(\mathbf{z}, \mathbf{y}) = (1/2)d(\mathbf{x}, \mathbf{y})$.

convex metric in any circle about the origin for any value of $2N_0$. The question remains open as to whether or not $d(\mathbf{z}, \mathbf{s})$ admits an accurate convex metric approximation in a neighborhood of the origin. Appendix B reports the results of an investigation of this question.

By considering the above properties, it is apparent that a signal constellation will be relatively immune to small amounts of phase jitter either if the error rate (or minimum distance) is determined by a point at the origin and any other signal point, or if signal points on the same circle are widely separated (the more circles the greater the Gaussian noise penalty).

2.5 *Probability Density in the Absence of a Phase-Locked Loop*

In a subsequent section we will compare the performance of various signal constellations, and the following question naturally arises: Can we, by judicious signal design, eliminate the need for a phase-locked loop?* Preliminary to answering this question we must obtain the density of the demodulated signal in the absence of a phase-locked loop. For simplicity we model the jitter as arising from the single tone

$$\phi(t) = A \cos(\omega_j t + \psi), \tag{20}$$

where $2A$ is the peak-to-peak jitter, ω_j is the jitter frequency, and ψ is a uniformly distributed random phase. For this model, the jitter density is given by

$$p(\phi) = \begin{cases} \dfrac{1}{A\pi\sqrt{1 - \left(\dfrac{\phi}{A}\right)^2}} & |\phi| \leqq A \\ 0 & |\phi| > A \end{cases}. \tag{21}$$

To determine the density of the demodulated samples we use (9) and (10) to write

$$p_j(\mathbf{z}) = \frac{1}{2\pi N_0} \exp\left\{-\frac{1}{2N_0}\left[\|\mathbf{z} - \mathbf{s}^{(j)}\|^2 + 2\langle \mathbf{z}, \mathbf{s}^{(j)}\rangle\right]\right\} \times \int_{-A}^{A} \exp\left\{\frac{1}{N_0}\left[(\mathbf{z}, \mathbf{s}^{(j)}) \cos\phi + \langle \mathbf{z}, \mathbf{s}^{(j)}\rangle \sin\phi\right]\right\} p(\phi)d\phi$$

which for small (<12 degrees) peak-to-peak jitter becomes

$$p_j(\mathbf{z}) \approx \frac{1}{2\pi N_0} \exp\left[-\frac{1}{2N_0}\|\mathbf{z} - \mathbf{s}^{(j)}\|^2\right] M_\phi(\xi_j), \tag{22}$$

* The equalizer[4] is capable of determining the optimum demodulating static phase, so that the demodulation is noncoherent only to the degree that the untracked jitter degrades the error rate.

where $M_\phi(\cdot)$ is the moment-generating function of ϕ, and

$$\xi_j = \frac{1}{N_0}(\mathbf{z}, \mathbf{s}^{(j)\perp}). \tag{23}$$

For the jitter density given by (21) it is easy to show that

$$M_\phi(\xi_j) = I_0(A\,|\,\xi_j|); \tag{24}$$

thus we have the familiar form

$$p_j(\mathbf{z}) = \frac{1}{2\pi N_0} \exp\left[-\frac{1}{2N_0} D^2(\mathbf{z}, \mathbf{s}^{(j)})\right], \tag{25}$$

where

$$D^2(\mathbf{z}, \mathbf{s}) = \|\mathbf{z} - \mathbf{s}\|^2 - 2N_0 \ell\text{n}\, I_0\left(\frac{A}{N_0}\,|(\mathbf{z}, \mathbf{s}^{(j)\perp})|\right). \tag{26}$$

It is useful to summarize our work up to this juncture. Using the simple model (4) and the phase-error densities (7) and (21), we have derived the conditional density of the demodulated two-tuple with and without a phase-locked loop. Equations (13) and (14) and (25) and (26) are the desired expressions. In the next section we will use these densities to estimate the system error rate.

III. ESTIMATING THE ERROR RATE

In this section we give two estimates of the error rate: an asymptotic (high SNR) evaluation and an upper bound. Consider the arbitrary signal constellation shown in Fig. 7, where the decision regions are denoted by R_j. The detector, which is specified by the decision regions, will declare that $\mathbf{s}^{(j)}$ has been transmitted if and only if the demodulated vector $\mathbf{z}$ falls inside R_j. Because of various practical considerations, principally ease of implementation, the mathematically optimum detector will not always be the one which is built.

3.1 *Asymptotic (High SNR) Error Rate*

The probability of error is given by

$$P_e = \sum_{j=1}^{M} p_j P_{ej}, \tag{27}$$

where the p_j's are the (taken to be equal) *a priori* probabilities and P_{ej} is the conditional error rate. The conditional error rate is just the probability that $\mathbf{z}$ falls outside R_j when $\mathbf{s}^{(j)}$ is transmitted, i.e.,

$$P_{ej} = \Pr\left[\mathbf{z} \notin R_j \,|\, \mathbf{s}^{(j)} \text{ transmitted}\right]. \tag{28}$$

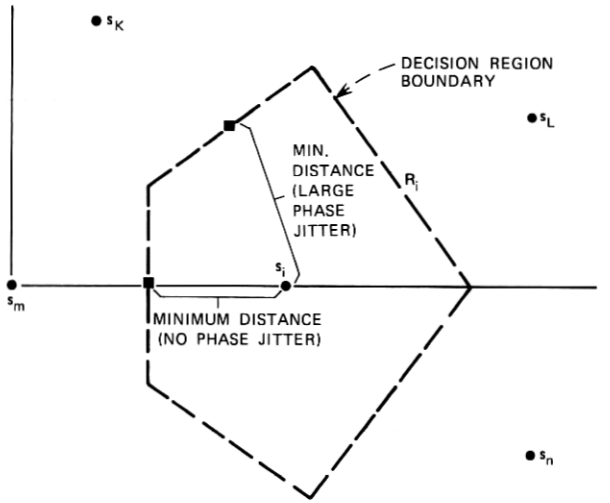

Fig. 7—Typical decision region about signal point $\mathbf{s}_i$, with minimum distances to boundary shown for Gaussian noise alone (no phase jitter) and for large jitter (angular displacements highly likely).

This quantity may be written, using the conditional density $p_j(\mathbf{z})$, as

$$P_{ej} = \int_{\mathbf{z} \in R_j} p_j(\mathbf{z}) d\mathbf{z}. \tag{29}$$

Let $\mathbf{z}_j^*$ denote a point of global minimum for the function d^2 or D^2 on the decision region boundary and let M_j be the number of times this minimum is achieved on the boundary. Let (u, v) denote an orthogonal coordinate system erected at $\mathbf{z}_j^*$ with the positive u axis pointed along the boundary line in a clockwise direction and v pointed outside R_j. Then, as is shown in Appendix A, for a high signal-to-noise ratio ($N_0 \to 0$) with $\alpha N_0 = k$, the conditional error rate is given by

$$P_{ej} = \frac{M_j}{\dfrac{\partial d^2}{\partial v}} \sqrt{\frac{N_0}{2\pi \left| \dfrac{\partial^2 d^2}{\partial u^2} \right|}} \cdot \exp \left. \frac{-d^2}{2N_0} \right|_{\mathbf{z}=\mathbf{z}_j^*}. \tag{30a}$$

For the case of Gaussian noise alone (no phase jitter) d^2 becomes the ordinary Euclidean distance and the partials in (30a) are easily evaluated. In this case, with $\mathbf{s}^{(i)}$ the signal(s) closest to $\mathbf{s}^{(j)}$, we have

$$\mathbf{z}_j^* = \frac{\mathbf{s}^{(i)} + \mathbf{s}^{(j)}}{2}$$

and

$$\left.\frac{\partial d^2}{\partial v}\right|_{z=z_j^*} = \|\mathbf{s}^{(i)} - \mathbf{s}^{(j)}\|$$

$$\left.\frac{\partial^2 d^2}{\partial u^2}\right|_{z=z_j^*} = 2.$$

Hence, for the Gaussian case,

$$P_{ej} = \frac{M_j}{2\|\mathbf{s}^{(i)} - \mathbf{s}^{(j)}\|}\sqrt{\frac{N_0}{\pi}}\exp\frac{-\|\mathbf{s}^{(i)} - \mathbf{s}^{(j)}\|^2}{8N_0}, \tag{30b}$$

a useful formula in its own right.

In terms of the distance functions $d(\cdot)$ and $D(\cdot)$, the asymptotic error rate is determined by the point on the decision boundary "closest" to the transmitted signal. Of course, in the presence of phase jitter, this point will generally differ from the closest point according to a Euclidean measurement. In Fig. 7, the indicated point on the vertical boundary segment is the closest point to $\mathbf{s}_j$ in the Euclidean sense. As phase jitter increases, those points with a radial coordinate nearly equal to that of $\mathbf{s}_j$ becomes closer to $\mathbf{s}_j$. So for large phase jitter, the point indicated on the boundary segment above $\mathbf{s}_j$ is the "closest" point. Thus the exponential decay in error rate is quite similar to the asymptotic Gaussian result since it is of the form

$$\exp\left[-d_{\min}^2(j)/2N_0\right], \tag{31}$$

where $d_{\min}(j)$ is the *minimum distance* (measured in a non-Euclidean manner) to the jth decision boundary. The minimum distance can sometimes be obtained analytically, but most often must be obtained by a computer search of the boundary.

The minimum distance to the jth decision boundary is particularly easy to determine if the function $d(\cdot,\cdot)$ is a metric which possesses the midpoint property, i.e., for each distinct pair of points $\mathbf{s}^{(i)}$ and $\mathbf{s}^{(j)}$ there exists a third point $\mathbf{z}^*$ such that

$$\tfrac{1}{2}d(\mathbf{s}^{(i)}, \mathbf{s}^{(j)}) = d(\mathbf{s}^{(i)}, \mathbf{z}_*) = d(\mathbf{z}_*, \mathbf{s}^{(j)}).$$

If this is the case, let $\mathbf{z}_i$ denote any point on the decision boundary between $\mathbf{s}^{(i)}$ and $\mathbf{s}^{(j)}$ and the triangle inequality gives

$$d(\mathbf{s}^{(j)}, \mathbf{z}_i) + d(\mathbf{s}^{(i)}, \mathbf{z}_i) \geqq d(\mathbf{s}^{(i)}, \mathbf{s}^{(j)}). \tag{32a}$$

Since for maximum-likelihood detection

$$d(\mathbf{s}^{(j)}, \mathbf{z}_i) = d(\mathbf{s}^{(i)}, \mathbf{z}_i),$$

minimizing both sides of (32a) over the decision boundary gives

$$d(\mathbf{s}^{(j)}, \mathbf{z}^*) \geqq \min_{i \neq j} \tfrac{1}{2} d(\mathbf{s}^{(i)}, \mathbf{s}^{(j)}) \tag{32b}$$

where $\mathbf{z}^*$ is the point on the boundary closest to $\mathbf{s}^{(j)}$. Note that (32b) would provide an upper bound on (31). Since the midpoint $\mathbf{z}^*$ clearly lies on the boundary, $\mathbf{z}^* = \mathbf{z}_*$, and (32b) is satisfied with equality, the minimum distance is given by

$$d(\mathbf{s}^{(i)}, \mathbf{z}^*) = \min_{j \neq i} \tfrac{1}{2} d(\mathbf{s}^{(i)}, \mathbf{s}^{(j)}). \tag{32c}$$

Since the Euclidean metric is convex, eq. (30b) could be directly obtained from (30a) by using (32c).

3.2 *An Upper Bound on the Error Rate (for Small Jitter)*

In systems which use a tracking loop, an upper bound on the system error rate may be obtained, for small jitter, by considering Fig. 8. This figure shows the transmitted point $\mathbf{s}^{(j)}$, the decision boundary R_j, and several nested regions C_j (defined by contours of constant probability), where

$$C_j = \{\mathbf{z} : d^2(\mathbf{z}, \mathbf{s}^{(j)}) \leqq c_j\}.$$

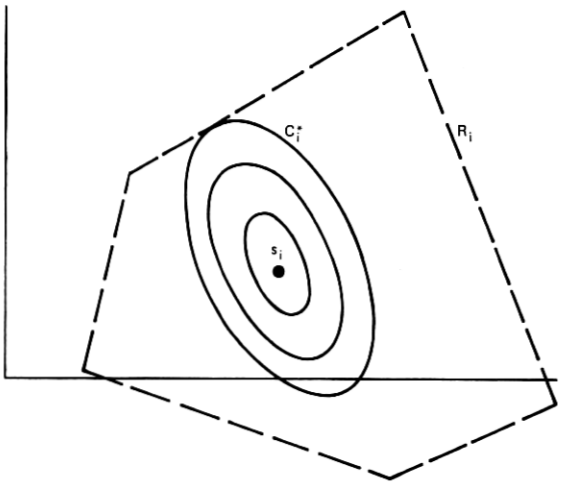

Fig. 8—Nested equidistance contours [distance defined by eq. (13)] about signal $\mathbf{s}_i$ in arbitrary decision region. Contour c_i^*, at distance d_i^*, defines d_i^* as the shortest distance to the boundary.

If we let C_j^* denote the first contour which touches the boundary, then it is clear that

$$P_{ej} = \Pr[\mathbf{z} \notin R_j | \mathbf{s}^{(j)} \text{ transmitted}] \leqq \Pr[\mathbf{z} \notin C_j^* | \mathbf{s}^{(j)}]$$

$$= \int_{\mathbf{z} \notin C_j^*} p_j(\mathbf{z}) d\mathbf{z}$$

$$= \int_{d^2\{\mathbf{z}, \mathbf{s}^{(j)}\} \geq c_j^{*2}} \exp\left[-\frac{1}{2N_0} d^2(\mathbf{z}, \mathbf{s}^{(j)}) \right] d\mathbf{z}. \tag{33}$$

For small jitter, the exponent may be expanded in the first power of $1/\alpha$, to give

$$d^2(\mathbf{x}, \mathbf{s}) = \|\mathbf{x} - \mathbf{s}\|^2 - \frac{1}{\alpha N_0} \langle \mathbf{x}, \mathbf{s}^1 \rangle^2, \tag{34}$$

for which the contours of constancy are ellipses. Transforming the ellipses into circles and changing to polar coordinates enable us to integrate (33) to get

$$P_{ej} \leqq \frac{1}{\sqrt{1 - \frac{\|\mathbf{s}^{(j)}\|^2}{\alpha N_0}}} \exp[-d_{\min}^{(j)2}/2N_0]. \tag{35}$$

Again $d_{\min}^{(j)}$ is the minimum distance to the jth decision boundary which for convex polygonal decision boundaries can be determined analytically. For high SNR, the above bound is useful up to 1.5 degrees rms jitter. Because of the similarity of (30a) and (35), we will use only the former asymptotic results in the sequel.

IV. A COMPARISON OF VARIOUS SIGNAL CONSTELLATIONS

In the preceding section we have presented a means of evaluating the asymptotic (high SNR) error rate for a given signal constellation and detector structure. In terms of the minimum distance, measured via the appropriate noise/phase-jitter distance function to the jth decision boundary, we have

$$P_e \sim \sum_j p_j \frac{M_j}{2\|\mathbf{s}^{(i)} - \mathbf{s}^{(j)}\|} \sqrt{\frac{N_0}{\pi}} \exp\left[-\frac{1}{2N_0} d_{\min}^{(j)2} \right]. \tag{36}$$

The minimum distance will be obtained by a computer search of the decision boundary. It should be emphasized that comparisons based on the asymptotic error rate are not exact but rather indicate order-of-magnitude effects.

Our comparisons will be made by varying the following quantities:

(*i*) signal constellations
(*ii*) signal-to-noise ratios
(*iii*) rms jitter
(*iv*) decision boundaries
(*v*) phase-error density.

Clearly the pie may be sliced several ways, so let us first say a few words about each of the above variables.

(*i*) *Signal constellations*: For the purposes of signal evaluation we will consider the existing 16-point constellations QAM, 8–8, and (4, 90°) shown in Figs. 9a through 9c. The circular constellation (4, 90°) has signal points equally spaced (i.e., 90 degrees apart) on four circles. This large angular spacing of points on the same circle suggests that this constellation will be insensitive to small amounts of phase jitter. The ratio of outer radius to inner radius (r_2/r_1) for the 8–8 constellation is 1.59, found by Lucky[1] to minimize the error rate in Gaussian noise. 8–8 is an optimized form of AM-PM in which signal points on the outer circle do not lie on the same radial lines as those on the inner circle. It offers an order-of-magnitude improvement (over AM-PM) in error rate in the presence of Gaussian noise. We will also consider the new circular modulation formats 1–5–10, 1–6–9, 5–11, shown in Fig. 10. The optimum ratio (r_2/r_1) is very close to 2 for these constellations as we have determined by equating the three smallest nearest-neighbor distances.

(*ii*) We consider peak and average SNR's, P_{pk} and P_{avg} respectively, chosen so that P_e (no jitter) is $<10^{-5}$. These quantities are

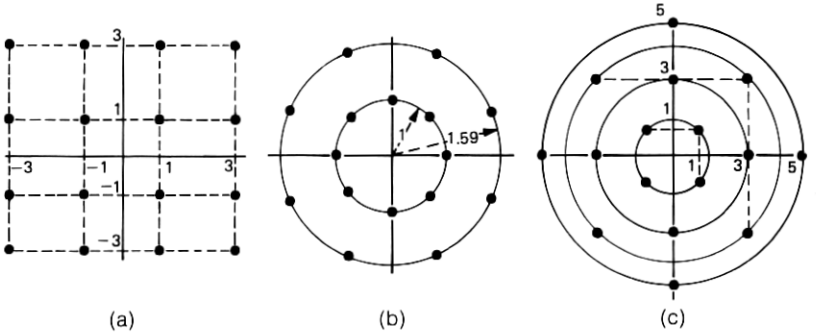

Fig. 9—Existing signal constellations: (a) quadrature amplitude modulation (QAM), $p_{peak}/p_{av} = 1.8$; (b) modified AM-PM (8–8), $p_{peak}/p_{av} = 1.43$; (c) circular constellation, (4, 90°) $p_{peak}/p_{av} = 1.85$.

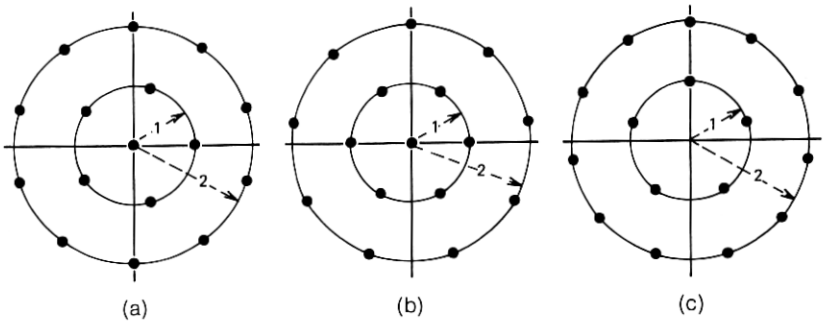

Fig. 10—New signal constellations: (a) 1–5–10, $p_{peak}/p_{av} = 1.42$; (b) 1–6–9, $p_{peak}/p_{av} = 1.525$; (c) 5–11, $p_{peak}/p_{av} = 1.31$.

defined by

$$P_{pk} = \max_{j} \|\mathbf{s}^{(j)}\|^2/2N_0,$$

$$P_{avg} = \frac{1}{16}\sum_{j=1}^{16} \|\mathbf{s}^{(j)}\|^2/2N_0.$$

(*iii*) Our attention is focused on the practical range of residual (from a PLL) jitter of <3 degrees rms.

(*iv*) We will consider both the boundaries which are optimum in Gaussian noise (straight lines) as well as more practical boundaries for the circular formats (polar wedges).

(*v*) The Tikhonov density will be taken as representative of those systems which use a tracking loop, while the peak-to-peak density will be used to model the raw (untracked) phase jitter.

The error rate curves are grouped as follows: Figure 11 shows the error rate vs rms residual phase jitter (Tikhonov density) under average and peak power constraints for the six constellations described above. For each constraint, a Gaussian noise power (and thus an SNR) is assumed which places the curves in a useful operating range, and the receiver is presumed to use the Gaussian optimum decision region boundaries. These boundaries are piecewise-linear contours constructed from segments of perpendicular bisectors of lines joining signal points as shown in Fig. 12a for the 1–5–10 constellation. This is equivalent to deciding in favor of the signal point closest in Euclidean distance to the demodulated point. Figure 12b shows a more "practical" set of decision boundaries for the 1–5–10 constellation. Figure 11 indicates the immunity of the (4, 90°) constellation to small amounts of phase jitter at the expense of an error rate more than an order of magnitude greater

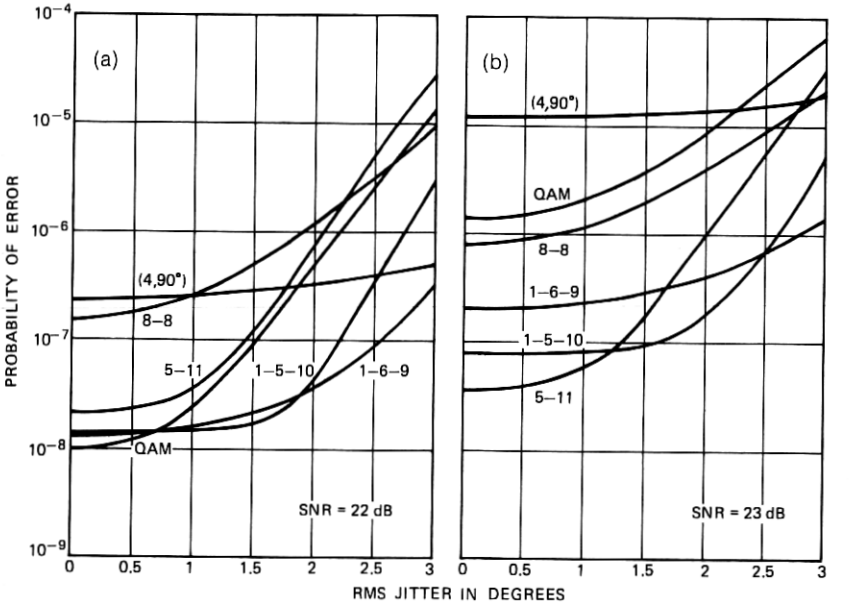

Fig. 11—Error rate vs jitter with a phase-locked loop: (a) average power constraint; (b) peak power constraint.

than those of the 1–5–10, 1–6–9, and QAM constellations. In practical operation with a tracking loop, any of these alternative constellations will almost always outperform the (4, 90°) constellation.

Figure 13 shows the error rates vs SNR, again under average and peak power constraints, in the presence of Gaussian noise alone (no phase jitter) and with 1.5 degrees rms residual phase jitter in addition

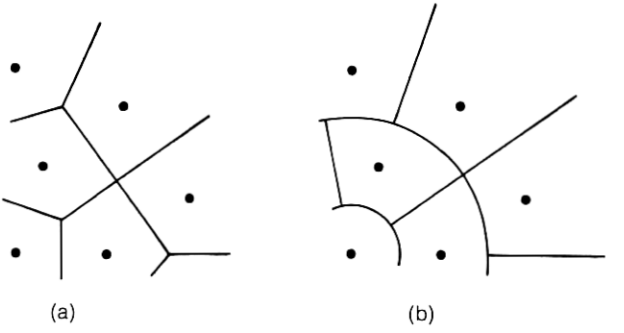

Fig. 12—Decision region boundaries for part of 1–5–10 constellation: (a) Gaussian-optimum decision region boundaries; (b) practical decision region boundaries.

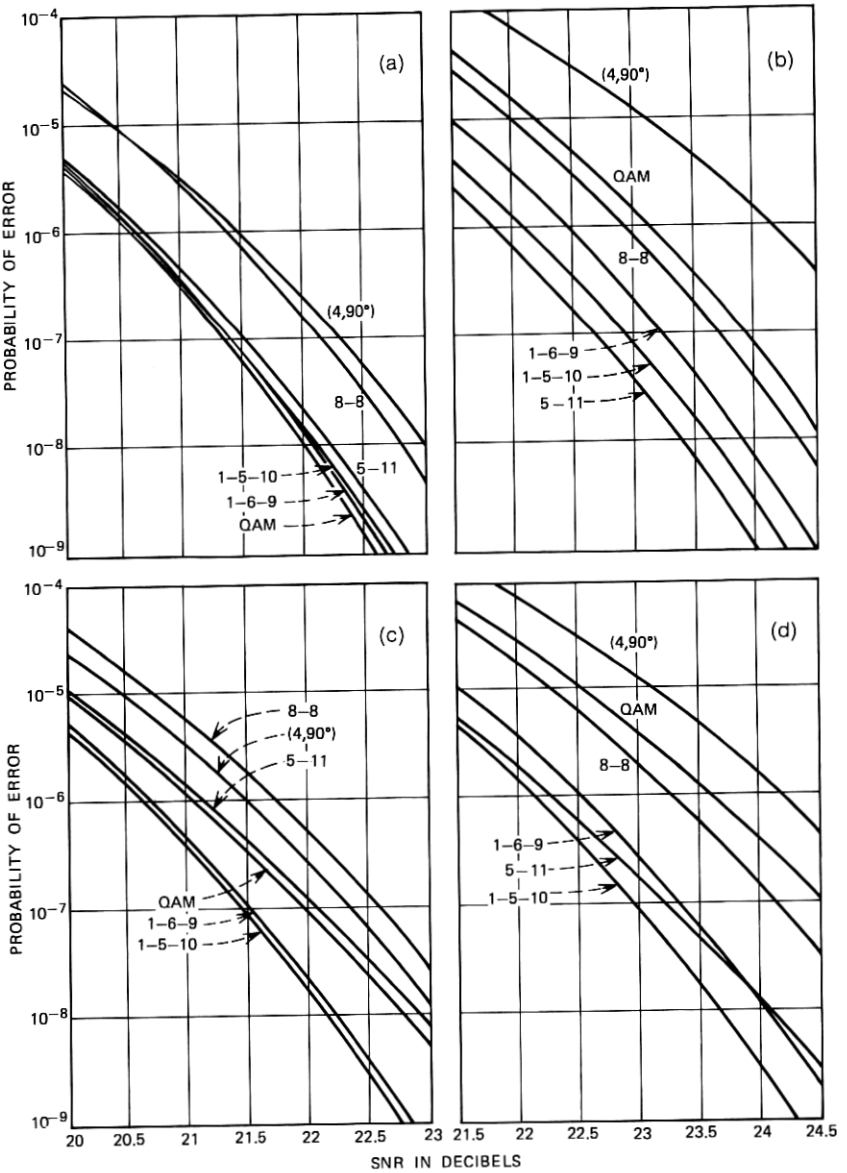

Fig. 13—Error rate vs SNR for channels with and without phase jitter; Gaussian-optimum receiver is assumed to have a phase-locked loop: (a) no jitter, average power constraint; (b) no jitter, peak power constraint; (c) rms jitter = 1.5 degrees, average power constraint; (d) rms jitter = 1.5 degrees, peak power constraint.

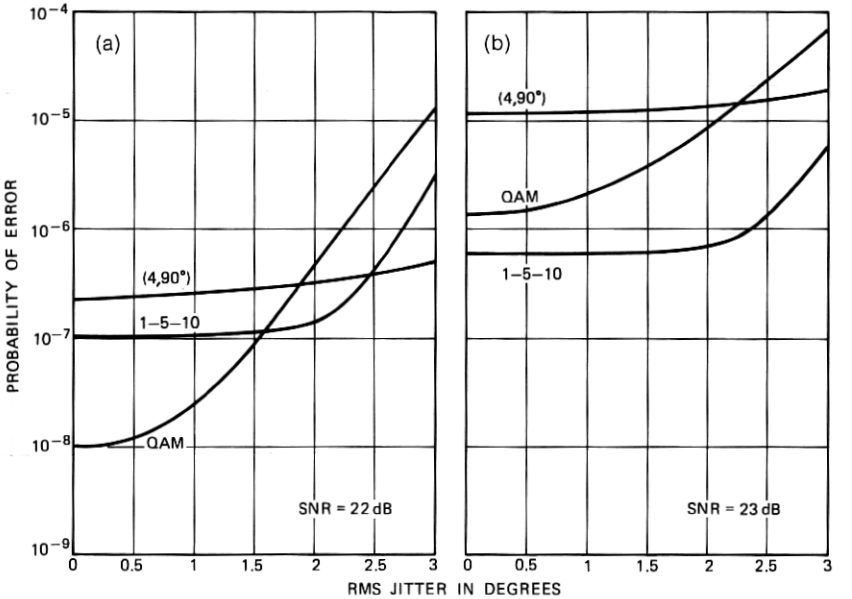

Fig. 14—Probability of error for receiver with "practical" decision region boundaries for the 1–5–10 constellation and with phase-locked loop: (a) average power constraint; (b) peak power constraint.

to the Gaussian noise. Although some of the curves shift their relative positions (at least under the average power constraint) when phase jitter is added, the good performances of 1–5–10 and 1–6–9 are maintained. QAM performs respectably and the (4, 90°) constellation comes in last.

Figure 14 is similar to a reduced Fig. 11 except that the "practical" set of decision region boundaries is presumed for the 1–5–10 constellation. As can easily be seen, the Gaussian optimum boundaries for QAM are also practical boundaries, and the jitter-immune (4, 90°) constellation is shown to best advantage by presuming Gaussian optimum boundaries. Under the average power constraint, QAM is superior to 1–5–10 below about 1.5 degrees rms jitter. Under the peak power constraint, 1–5–10 is uniformly superior to QAM. The (4, 90°) constellation does not show an advantage until the rms jitter reaches 2.5 to 3 degrees.

Figure 15 is a set of error rate vs SNR plots with practical decision region boundaries for 1–5–10. Curves are shown for Gaussian noise alone (no jitter) and 1.5 degrees rms jitter. Only the average power

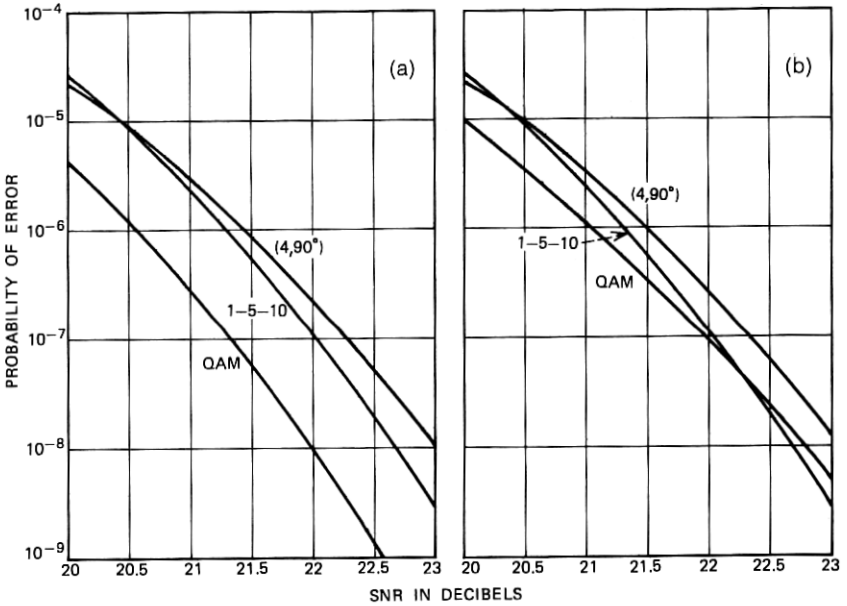

Fig. 15—Probability of error vs SNR for Gaussian-optimum receiver with "practical" decision region boundaries for the 1–5–10 constellation and with phase-locked loop: (a) no jitter, average power constraint; (b) rms jitter = 1.5 degrees, average power constraint.

constraint is presumed. As before, QAM shows an advantage in the absence of phase jitter and still does well in the presence of moderately severe residual phase jitter.

Figure 16 presents some data for receivers which do not use tracking loops. In this case the peak-to-peak density of eq. (22) describes the raw jitter. Curves are plotted vs peak jitter under average and peak power constraints. Some interesting features are the resistance of 1–5–10 up to a threshold of about 8 degrees peak-to-peak jitter and the rapid deterioration of the performance of QAM.

Figure 17 shows the performance vs SNR for the receivers without tracking loops when the peak-to-peak jitter is 12 degrees. This is the only instance for which the (4, 90°) constellation looks relatively good, but here, too, the 1–6–9 constellation performs slightly better. QAM, of course, does rather poorly.

The advantage of using a phase-locked tracking loop with QAM and 1–5–10 can be seen from the above data and a simple calculation. If the raw phase jitter is modeled by

$$Q(t) = A \cos [\omega_j t + \psi],$$

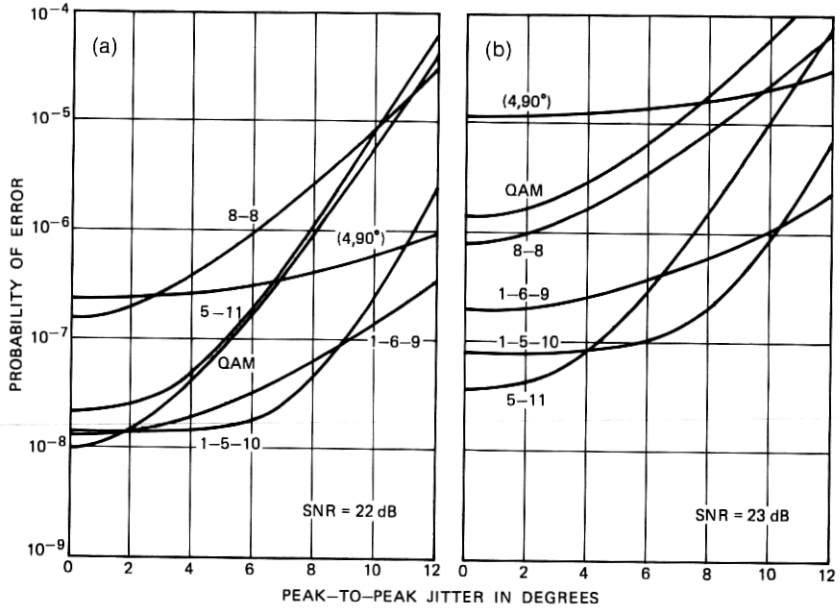

Fig. 16—Probability of error vs. peak-to-peak jitter for Gaussian-optimum receiver without a phase-locked loop: (a) average power constraint; (b) peak power constraint.

where ψ is uniformly distributed from $-\pi$ to π and $2A$ is the peak-to-peak jitter, then a rule of thumb[9] suggests that the residual rms jitter out of a tracking loop is of the order of $0.1 \times 2A$. For $A = 6$ degrees, this rms value is 1.2 degrees. A comparison of the curves of Figs. 11 and 16 shows that substantially lower error rates are achieved by the receiver with a tracking loop. The performance of constellation (4, 90°) is relatively unaffected by the introduction of a tracking loop.

A further conclusion that can be drawn from the numerical data is that the QAM constellation, which is simple to generate and to demodulate, performs quite well in Gaussian noise alone or (with the aid of tracking loop) Gaussian noise plus phase jitter. More circular constellations, such as 1–5–10 and 1–6–9, appear to offer a moderate further advantage at the expense of greater complexity.

V. OPTIMUM SIGNAL CONSTELLATIONS UNDER A PEAK POWER CONSTRAINT

In this section we discretize the received signal space to obtain a tractable optimization problem. The discretizing is such that the M signal points are selected from a circle containing L points while the received points lie in a circle of N ($N > L$) points (note: $M < L$). We make the following two comments concerning this approach to solving

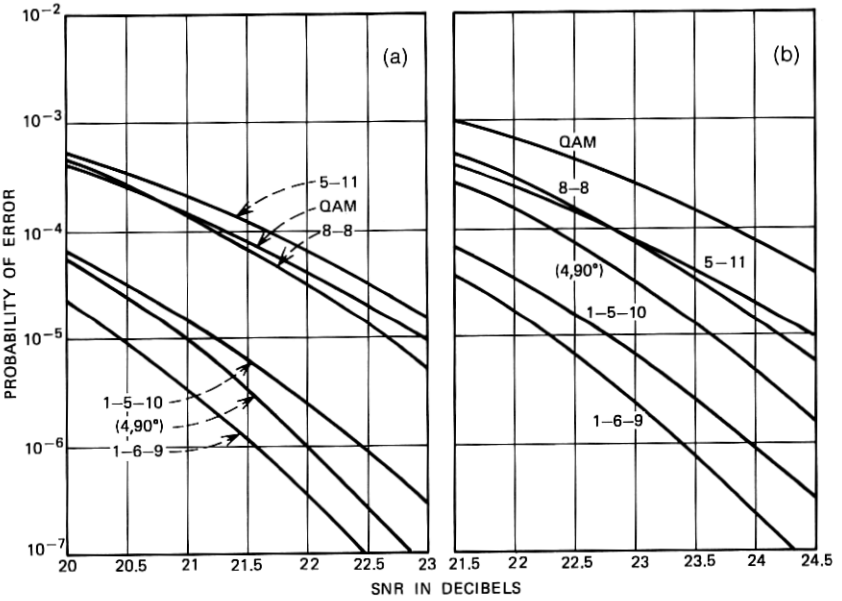

Fig. 17—Probability of error vs SNR for Gaussian-optimum receiver without a phase-locked loop: (a) peak-to-peak jitter = 12 degrees, average power constraint; (b) peak-to-peak jitter = 12 degrees, peak power constraint.

the problem:

(*i*) the level of discretization must be fine enough to provide a good approximation to the continuous problem, and

(*ii*) the outer radius must be chosen so that for all practical purposes the probability that a received point lies outside the outer circle is negligible. The peak power constraint simply means that no signal points can be selected outside the L circle.

5.1 *Discrete Maximum-Likelihood Formulation*

If we denote the received point, $\mathbf{z}$, by "i" and the transmitted signal, $\mathbf{s}^{(j)}$, by "j," then the perturbation of the transmitted signal due to Gaussian noise and phase jitter may be summarized by a transition matrix whose elements are defined by

$$\begin{aligned} p(i\,|\,j) &= \Pr\,[\text{receiving } \text{“}i\text{”}\,|\,\text{transmitting } \text{“}j\text{”}] \\ i &= 1, 2, \cdots N \\ j &= 1, 2, \cdots M. \end{aligned} \tag{37}$$

The transition probabilities may be computed by integrating the condi-

tional densities $p_j(\mathbf{z})$ over an appropriate region. It is convenient to work with the maximum-likelihood receiver (i.e., the optimum decision boundaries are used) which receives "i" and declares that "ℓ_i" was transmitted, where

$$p(i|\ell_i) > p(i|j), \; j \neq \ell_i \qquad j, \ell_i = 1, 2, \cdots M. \tag{38}$$

Note that we have (temporarily) fixed the M points in the signal constellation. It is easy to see that the probability of being correct is given by

$$\Pr[\text{correct}] = \sum_{i=1}^{N} \Pr[\text{correct}|\text{receive } "i"] \Pr[\text{receive } "i"], \tag{39}$$

but by Bayes rule

$$\begin{aligned}\Pr[\text{correct}|\text{receive } "i"] &= \Pr[\text{send } "\ell_i"|\text{receive } "i"] \\ &= \frac{\Pr[\text{receive } "i"|\text{send } "\ell_i"] \Pr[\text{send } "i"]}{\Pr[\text{receive } "i"]}.\end{aligned} \tag{40}$$

Substituting (40) in (39) and recalling that the transmitted signals are equiprobable gives

$$\begin{aligned}\Pr[\text{correct}] &= \frac{1}{M} \sum_{i=1}^{N} \Pr[\text{receive } "i"|\text{send } "\ell_i"] \\ &= \frac{1}{M} \sum_{i=1}^{N} p(i|\ell_i),\end{aligned} \tag{41}$$

and the optimum constellation is the M signals (or columns) that maximize

$$\sum_{i=1}^{N} p(i|\ell_i). \tag{42}$$

Note that since $p(i|\ell_i)$ is the maximum entry in the ith row of the transition matrix, the problem is one of selecting M out of L columns such that the sum of the row maxima is maximized. The error rate may be determined from (41).

5.2 *Optimum Constellations*

A heuristic program for solving the combinational optimization problem posed by (42) has been developed by Kernighan and Lin.[6] Their process is based upon iterative improvement of either known initial constellations or random initial starts. For each start, a "locally

optimum" solution is found in the sense that no change of position of a single signal can improve the criterion. The heuristic process is very fast and, for the resolution we require, 20 random starts can be pursued to completion in 25 seconds. For particular values of rms phase jitter and noise power we find, among the best of 20 local optima, reaffirmation of known solutions and in some instances new competitive constellations. For example, for a peak signal energy of SNR = 22 dB, Figs. 18, 19, and 20 give the best among the 20 local optima for an rms of 0, 1.5, and 3 degrees, respectively. As expected, the 0-degree solution has a 5–11 character and the 1.5-degree solution has a 1–5–10 character. On the other hand, the 3-degree solution is somewhat of a surprise; it has a 1–6–9 character. The (4, 90°) constellation, which is

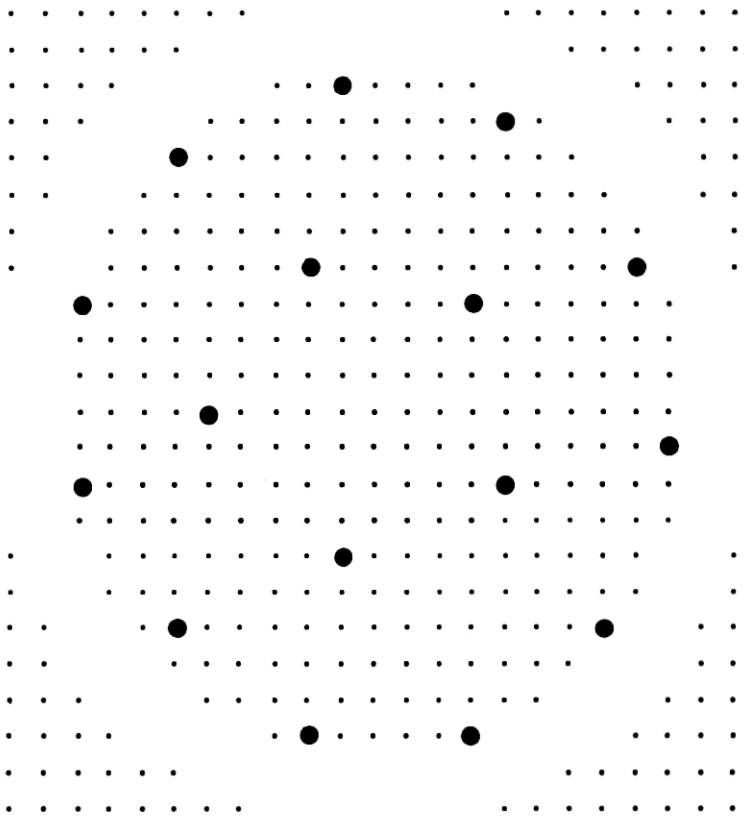

Fig. 18—Optimum signal constellation: Peak SNR = 27 dB, no jitter (courtesy of B. W. Kernighan and S. Lin).

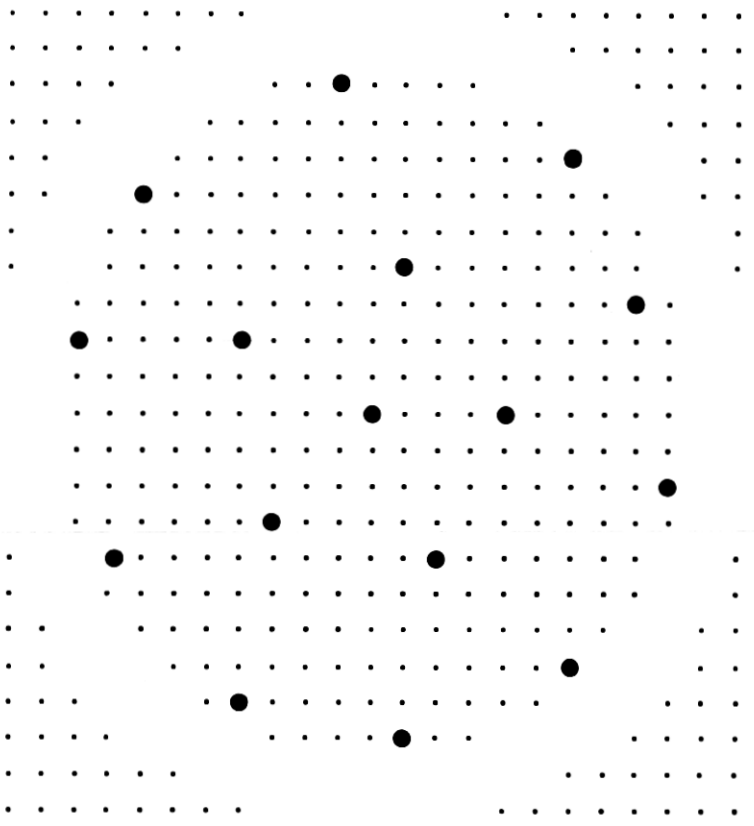

Fig. 19—Optimum signal constellation: Peak SNR = 27 dB, 1.5 degrees rms jitter (courtesy of B. W. Kernighan and S. Lin).

best at 3 degrees among heretofore considered designs, has an error rate only a few percent worse than that of the 1–6–9 constellation.

A byproduct of the development of the above procedure is the demonstration of the fact that numerical quadrature routines offer a competitive alternative to asymptotic techniques and bounding methods for the estimation of system error rates.

VI. CONCLUSIONS

Comparisons have been made of several well-known two-dimensional signal formats in the presence of Gaussian noise and phase jitter, at high signal-to-noise ratios and under both peak and average power constraints. It has been demonstrated that, under an average

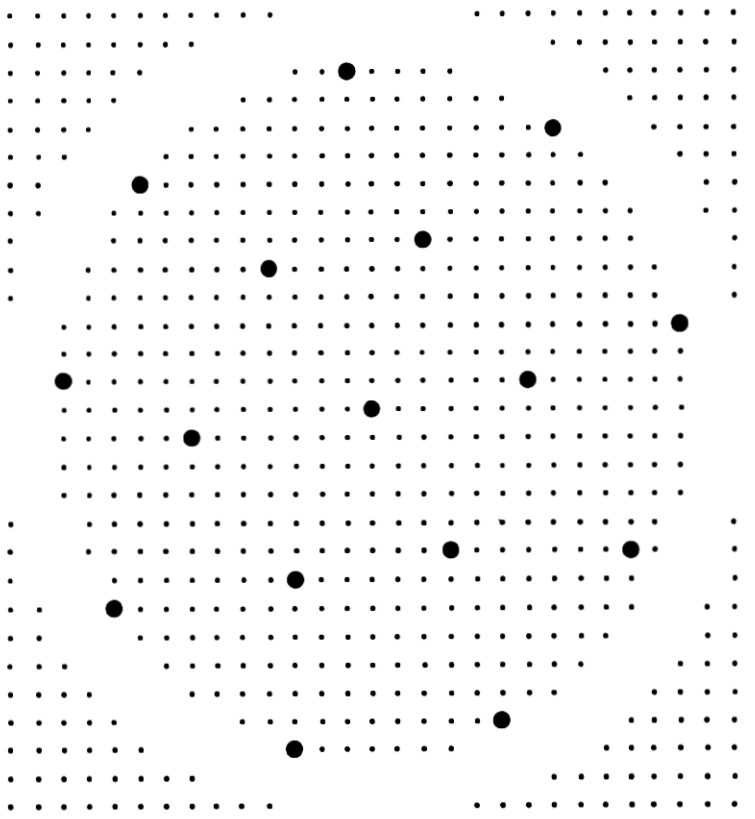

Fig. 20—Optimum signal constellation: Peak SNR = 27 dB, 3 degrees rms jitter (courtesy of B. W. Kernighan and S. Lin).

power constraint for systems which have a high-quality phase-locked loop (rms residual jitter <1 degree), QAM had the lowest error rate of all candidate constellations. If the residual jitter is <1.5 degrees rms, the 1–5–10 constellation becomes extremely attractive since it is immune to phase jitter in this range and provides the same asymptotic (no-jitter) error rate as QAM. For small amounts of jitter, 1–5–10 and QAM have a 2-dB SNR advantage over the (4, 90°) constellation which is "immune" to phase jitter. Both these constellations offer a 0.5-to-1-dB advantage in SNR over conventional AM/PM signaling techniques. Thus, under an average power constraint, both QAM and 1–5–10 merit consideration.

For a peak power constraint, in addition to making comparisons similar to the above, we have been able to attain the optimum signal

constellations for various levels of jitter. Our comparisons indicate that, for jitter <1 degree, QAM suffers a 1.5-dB SNR penalty with respect to the 5–11 constellation, while 1–5–10 suffers a 0.1-dB penalty. At 1.5 degrees rms jitter, 1–5–10 again is superior to both QAM and 5–11 (by 4 and 1 dB respectively).

Based upon the peak and average power constraints, the new modulation format 1–5–10 appears to make extremely efficient use of available signal power and for a slight increase in modulation/demodulation complexity offers considerable immunity to moderate (<1.5 degrees rms) residual phase jitter. QAM systems which employ high-quality phase-locked loops will also be operating very efficiently, provided that the residual phase error is <0.8 degree rms.

VII. ACKNOWLEDGMENTS

We would like to thank J. Salz and J. E. Mazo for valuable discussions concerning this investigation.

APPENDIX A

Method of Laplace

Let $g(x)$ and $h(x)$ be continuous real functions on $[a, b]$ where $h(x)$ is also twice continuously differentiable. Then, if $h(x)$ attains a single maxima at c $(a < c < b)$, we have that

$$\int_a^b g(x)e^{(1/k)h(c)}dx \sim g(c)e^{(1/k)h(a)}\sqrt{\frac{-2\pi k}{h''(c)}} \qquad (k \to 0)$$

(read $\sim$ as asymptotic to). The proof is not difficult and the key steps can be found in Papoulis[10] or in Jones.[11] This analysis technique for estimating an integral for large values of the parameter k is called the method of Laplace.

An immediate application of this method used in the body of this paper is

$$I_0(\alpha) \triangleq \frac{1}{2\pi}\int_{-\pi}^{\pi} e^{\alpha\cos\theta}d\theta \sim \frac{e^{\alpha}}{\sqrt{2\pi\alpha}} \qquad (\alpha \to \infty).$$

For estimating system error rates, a certain two-dimensional version of Laplace's method is needed. Particularly, we shall investigate the following two-dimensional integral:

$$I \triangleq \iint_{v \geqq 0} \exp\left\{\frac{1}{k}h(\mathbf{z})\right\}d\mathbf{z} \qquad [\mathbf{z} = (u, v)]$$

for small k. The function $h(\mathbf{z})$ we shall be concerned with is assumed to have the following properties:

(*i*) $h(\mathbf{z})$ is twice continuously differentiable such that $h_v(\mathbf{0}) < 0$, $h_{uv}(\mathbf{0}) \neq 0$, and $\mathbf{0}$ is the unique point of maximum for $h(\mathbf{z})$ in $v \geqq 0$.* Thus we also assume h_{uu} of $(\mathbf{0}) < 0$.

Let $G_r = \{v \geqq 0,\ u^2 + v^2 \leqq r\}$

(*ii*) For some $r > 0$,

$$\lim_{k\to 0} \iint_{G_r} \exp\left\{\frac{1}{k} h(\mathbf{z})\right\} \Big/ I \to 1.$$

Rewriting I as

$$e^{(1/k)h(\mathbf{0})} \iint_{\{v\geqq 0\}} \exp\left\{\frac{1}{k}[h(\mathbf{z}) - h(\mathbf{0})]\right\},$$

it is easy to conclude that for each $\epsilon > 0$

$$I \sim e^{(1/k)h(\mathbf{0})} \int_{-\epsilon}^{\epsilon} \int_{0}^{\epsilon} \exp\left\{\frac{1}{k}[h(\mathbf{z}) - h(\mathbf{0})]\right\}.$$

We shall proceed to integrate with the exponent in the integrand replaced by its local representation

$$e^{(1/k)h(\mathbf{0})} \int_{-\epsilon}^{\epsilon} \int_{0}^{\epsilon} \exp\left\{\frac{1}{k}[h_v(\mathbf{0})v + h_{uu}(\mathbf{0})u^2/2 + h_{uv}(\mathbf{0})uv]\right\} dvdu.$$

The absence of $h_u(\mathbf{0})$ and $h_{vv}(\mathbf{0})$ follow directly from (*i*). Integrating (dv) we get

$$I \sim e^{(1/k)h(\mathbf{0})} \int_{-\epsilon}^{\epsilon} k \left\{\frac{\exp\left\{\frac{1}{k}[h_v(\mathbf{0})\epsilon + h_{uu}(\mathbf{0})u\epsilon]\right\} - 1}{h_v(\mathbf{0}) + h_{uv}(\mathbf{0})u}\right\} \times e^{(1/k(h_{uu}(\mathbf{0})(u^2/2)} du.$$

We appeal to the first paragraph to integrate each term involved in this subtraction. Take ϵ small enough to avoid the singularity at $u = -h_v(\mathbf{0})/h_{uv}(\mathbf{0})$. The first term is asymptotic to

$$k^{3/2} \sqrt{\frac{-2\pi}{h_{uu}(\mathbf{0})}} \left\{\exp \frac{1}{k}\left[h(\mathbf{0}) + h_v(\mathbf{0})\epsilon - \frac{h_{\mu\nu}^2}{h_{uu}} \epsilon^2\right]\right\}$$

* In this appendix, subscripts are used to denote partial derivatives, e.g., $h_v(\mathbf{0}) = \left.\frac{\partial h}{\partial v}\right|_{(u,v)=(0,0)}$.

while the second is

$$-\frac{k^{3/2}}{h_v(\mathbf{0})}\sqrt{\frac{-2\pi}{h_{uu}(\mathbf{0})}}\,e^{h(\mathbf{0})/k}.$$

Since for ϵ small enough $h_v(\mathbf{0})\epsilon - [h_{uv}^2(\mathbf{0})/h_{uu}(\mathbf{0})]\epsilon^2 < 0$, we conclude

$$I \sim \frac{-k^{3/2}}{h_v(\mathbf{0})}\sqrt{\frac{-2\pi}{h_{uu}(\mathbf{0})}}\,e^{h(\mathbf{0})/k}.$$

In error rate computations one is often integrating over the exterior of a convex polygon. In the body of this paper we encounter the case where $h(z)$ has a finite number of global maxima on the boundary, at most one on each side, and none at the vertices. Let $\mathbf{z}_n^*$ be the nth local maximum. Map the exterior half-space containing $\mathbf{z}_n^*$ into the upper-half plane via a rotation, composed with a translation taking $\mathbf{z}_n^* \to \mathbf{0}$. Then the method of the last paragraph can be applied. The process is repeated for each maxima and the results sum to the required asymptotic estimate of the exterior integral. The fact that the exterior half-spaces containing distinct points of maxima may overlap is of no consequence. Furthermore, in our applications, $h(\mathbf{z})$ is symmetric with respect to each $\mathbf{z}_k^*$ and the process need only be completed once and the answer multiplied by the multiplicity of the maxima.

APPENDIX B

The Nature of $d(x, y)$

B.1 *Introduction*

Let V be a vector space endowed with a scalar product $\langle \mathbf{x}, \mathbf{y}\rangle$ and a norm derived therefrom. It is not known whether $d_\gamma(\mathbf{x}, \mathbf{y})\colon V \times V \to |R|$ defined by

$$d_\gamma(x, y) = (\|\mathbf{x}\|^2 + \|\mathbf{y}\|^2 + 2\gamma^{-1} - 2|\sqrt{\|\mathbf{x}\|^2\|\mathbf{y}\|^2 + 2\gamma^{-1}\langle \mathbf{x}, \mathbf{y}\rangle + \gamma^{-2}}|)^{1/2}$$

is a metric for any values of γ $(0 < \gamma < \infty)$. Nor is it known whether $d_\gamma(\mathbf{x}, \mathbf{y})$ is a metric in any sphere centered about the origin. Similarly, the status of the midpoint property is also unknown to us. However, from Ref. 8, we know that these two properties cannot hold simultaneously for any γ in any sphere about the origin.

Concerning the metric question, the difficulty (as usual) is the triangle inequality. By definition $d_\gamma(\mathbf{x}, \mathbf{y})$ is symmetric in its arguments. Positivity follows easily from the Schwartz inequality,

$$d_\gamma(\mathbf{x}, \mathbf{y}) \geqq \{\|\mathbf{x} - \mathbf{y}\|^2 + 2\langle \mathbf{x}, \mathbf{y}\rangle + 2\gamma^{-1} - 2|\sqrt{\|\mathbf{x}\|^2\|\mathbf{y}\|^2 + 2\gamma^{-1}\|\mathbf{x}\|\|\mathbf{y}\| + \gamma^{-2}}|\} = |\,\|\mathbf{x}\| - \|\mathbf{y}\|\,| \geqq 0.$$

Notice $d_\gamma(\mathbf{x}, \mathbf{y}) > 0$ unless $x = y$. If $d_\gamma(x, y)$ is a metric on $V \times V$ for a particular value of γ then it is a metric for all γ $(0 < \gamma < \infty)$; this is easily obtained by employing the mapping $\mathbf{z} \to |\sqrt{\gamma}|\mathbf{z}$.

B.2 *One-Dimensional Case*

In the special case $V = R$ we can show $d_1(x, y)$ is a metric. In one dimension we have (the "1" subscript will now be suppressed)

$$d(x, y) = \begin{cases} |x - y| & xy + 1 \geqq 0 \\ |\sqrt{(x + y)^2 + 2^2}| & xy + 1 \leqq 0 \end{cases}.$$

To show the triangle inequality, first notice that, if three points a, b, and c are on the same side of zero, the distances are all Euclidean. So for the remaining cases to be investigated we assume one point has a different sign than the other two. Notice $d(x, y) = d(-x, -y)$ so we lose no generality by assuming $c \geqq b \geqq 0 \geqq a$. Two subcases remain: (i) only $d(c, a)$ is non-Euclidean; (ii) $d(c, a)$ and $d(b, a)$ are non-Euclidean. For (i) the distances involved are $(c - b)$, $(b - a)$, and $|[(a + c)^2 + 2^2]^{1/2}|$. Now $|[(a + c)^2 + 2^2]^{1/2}| \leqq c - a$ since, by squaring, this is equivalent to $1 + ac \leqq 0$. To show

$$(c - b) \leqq (b - a) + |[(a + c)^2 + 2^2]^{1/2}|$$

and

$$(b - a) \leqq (c - b) + |[(a + c)^2 + 2^2]^{1/2}|,$$

it is enough to show

$$[(c + a) - 2b]^2 \leqq [(a + c)^2 + 2^2]$$

since squaring both sides when the right-hand side is positive can only weaken the inequality. The last inequality can be simplified to $b^2 - bc \leqq 1 + ab$ for which the left-hand side is negative and the right-hand side is not. On the other hand, (ii) is immediate since $c - b$, $\sqrt{(a + c)^2 + 4}$, and $\sqrt{(b + a)^2 + 4}$ can be identified as sides of a triangle with apex $(-a, 2)$ and base points c and b. Notice d does not have the midpoint property since $d(10, -10) = 2$, yet the only points y satisfying $d(10, y) = 1$ are 9 and 11, but both $d(9, -10)$ $d(11, -10)$ exceed 2.

This last observation shows that the open spheres in this metric space are not all connected. In two dimensions, the boundaries of certain open spheres are disconnected; specifically, it can be shown that for certain values of $q > 0$

$$\{y \,|\, d(\mathbf{x}, \mathbf{y}) = q\}$$

is a disconnected set if $\|\mathbf{y}\|^2\gamma > 1$.

B.3 *Approximating $d_\gamma(x, y)$ on the Unit Circle*

As mentioned in the text, an important open question is whether $d_\gamma(x, y)$ can be accurately approximated by a convex metric. There are, of course, many ways in which one can approximate $d_\gamma(x, y)$. In this section we dispose of two approximations which suggest themselves immediately.

Let us view $d_\gamma(\mathbf{x}, \mathbf{y})$ on the unit circle. Notice, as $\gamma \to 0$,

$$|\sqrt{\|\mathbf{x}\|^2\|\mathbf{y}\|^2 + 2\gamma^{-1}\langle \mathbf{x}, \mathbf{y}\rangle + \gamma^{-2}}|$$
$$\approx \gamma^{-1}\left(1 + \gamma\langle \mathbf{x}, \mathbf{y}\rangle + \gamma^2\left(\frac{\|\mathbf{x}\|^2\|\mathbf{y}\|^2 - \langle \mathbf{x}, \mathbf{y}\rangle^2}{2}\right)\right).$$

Hence, for small phase jitter,

$$d_\gamma^2(x, y) \approx \|\mathbf{x} - \mathbf{y}\|^2 - \gamma\|\mathbf{x}\|^2\|\mathbf{y}\|^2 \sin^2\theta,$$

where θ is the angle between $\mathbf{x}$ and $\mathbf{y}$, or what is the same,

$$d_\gamma(\mathbf{x}, \mathbf{y}) \approx \|\mathbf{x} - \mathbf{y}\|\left(1 - 4\gamma\frac{A^2(\mathbf{x}, \mathbf{y})}{\|\mathbf{x} - \mathbf{y}\|^2}\right)^{1/2},$$

where $A(\mathbf{x}, \mathbf{y})$ is the area of the triangle $0xy$. Let h_{xy} denote the altitude of $0xy$ perpendicular to xy; then

$$d_\gamma(\mathbf{x}, \mathbf{y}) \approx \|\mathbf{x} - \mathbf{y}\|(1 - \gamma h_{xy}^2)^{1/2}.$$

Since $h \leqq 1$,

$$\|\mathbf{x} - \mathbf{y}\|(1 - \gamma h_{xy}^2)^{1/2} \geqq 0$$

with equality if and only if $\mathbf{x} = \mathbf{y}$ so long as $\gamma < 1$; also, the left-hand side is symmetric. Notice

$$\Delta(\mathbf{x}, \mathbf{y}) = \|\mathbf{x} - \mathbf{y}\|(1 - h_{xy}^2)^{1/2}$$

has the midpoint property. Indeed, if z lies on the line segment joining $\mathbf{x}$ and $\mathbf{y}$,

$$d(\mathbf{x}, \mathbf{z}) + d(\mathbf{z}, \mathbf{y}) = d(\mathbf{x}, \mathbf{y})$$

since $h_{xz} = h_{xy} = h_{yz}$.

So we are strongly motivated now to see if $\Delta(\mathbf{x}, \mathbf{y})$ is a metric on the unit disc. Note that if F is any finite subset of the unit disc, then for γ sufficiently small, $d(\mathbf{x}, \mathbf{y})$ is a metric on F. This follows from the fact that for noncolinear triples, the triangle inequality holds properly for the metric $\|\mathbf{x} - \mathbf{y}\|$. Perhaps surprisingly, the triangle inequality for $\Delta_\gamma(\mathbf{x}, \mathbf{y})$ does *not* hold for all triplets in the unit disc. This was discovered by linearizing $\Delta(\mathbf{x}, \mathbf{y})$ to get $\delta(\mathbf{x}, \mathbf{y}) = \|\mathbf{x} - \mathbf{y}\|(1 - \gamma/2h_{xy}^2)$ which is likewise a valid approximation for $d(\mathbf{x}, \mathbf{y})$ for small γ.

For $\delta(\mathbf{x}, \mathbf{y})$, the midpoint property and all requirements for a metric hold except for the triangle inequality. The triangle inequality question is easier for us to investigate for $\delta(\mathbf{x}, \mathbf{y})$ than for $\Delta(\mathbf{x}, \mathbf{y})$ as it develops into a geometrical extremal problem which we can handle. In solving the extremal problem, a class of vector triplets in the unit disc emerge for which no value of $\gamma > 0$ exists such that the triangle inequality holds uniformly for the class. Although these triplets arise in the analysis of $\delta(\mathbf{x}, \mathbf{y})$, they serve just as ruinously for $\Delta(\mathbf{x}, \mathbf{y})$.

In order to discuss this geometric extremal problem, we require some notation. Suppose we have a triangle (nontrivial—positive area) in the unit disc with side lengths a, b, and c and opposing vertices A, B, and C, respectively. Let h_a, h_b, and h_c denote the distance from the origin to the line containing the side of length a, b, and c, respectively.

Write the "triangle inequality" expression for $\delta(\mathbf{x}, \mathbf{y})$:

$$\|\mathbf{x} - \mathbf{y}\| \left(1 - \frac{r}{2} h_{xy}^2\right) \stackrel{?}{\leqq} \|\mathbf{x} - \mathbf{z}\| \left(1 - \frac{r}{2} h_{xz}^2\right) + \|\mathbf{z} - \mathbf{y}\| \left(1 - \frac{r}{2} h_{zy}^2\right).$$

Changing to the notation just introduced, we have directly that the triangle inequality holds for $0 \leqq \gamma \leqq \boldsymbol{\gamma}$ where $\boldsymbol{\gamma} = \inf \Gamma(a, b, c)$.

$$\Gamma(a, b, c) \triangleq \left\{ \frac{a + b - c}{a h_a^2 + b h_b^2 - c h_c^2} \right\}$$

and the infimum is over all triangles for which the bracketed expression is positive. This geometric extermal problem is disposed of by substituting a triangle of the form depicted in Fig. 21. It follows easily $\lim_{\epsilon \to 0} \Gamma = 0$. Thus $\boldsymbol{\gamma} = 0$ and the only $d(\mathbf{x}, \mathbf{y})$ metric is the obvious one. A straightforward substitution of the three vectors depicted above into the "triangle inequality" for $\Delta(\mathbf{x}, \mathbf{y})$ yields again that for no fixed $\gamma > 0$ can the triangle inequality hold for this family of triangles.

Strikingly, for the class of triplets in Fig. 21, it is easily demonstrated, via substitution, that the triangle inequality for $d_\gamma(x, y)$ holds for an open interval including $\gamma = 0$!

B.4 *A Metric on the Boundary of the Disc*

We end on a positive note: $\delta(x, y)$ is a metric on the boundary of the unit disc for a nontrivial interval $[0, \boldsymbol{\gamma}]$.* It is enough to show inf

* We anticipate applications in phase-modulation systems.

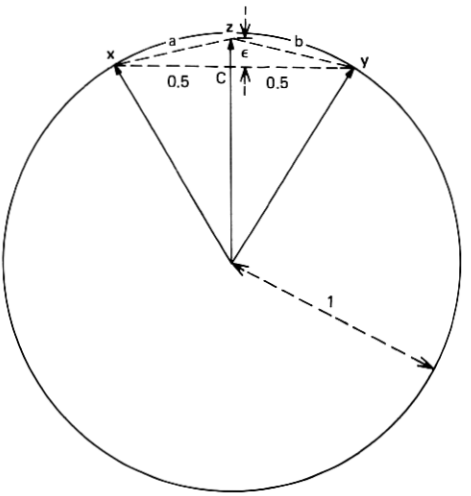

Fig. 21—Infimizing family of vectors.

$\Gamma(a, b, c) > 0$ where the infimum is over those triangles circumscribed by the unit circle for which Γ is positive. Now $h_a^2 = 1 - a^2/4$ and similarly for h_b and h_c so

$$\Gamma(a, b, c) = \left(1 - \frac{1}{4}\frac{a^3 + b^3 - c^3}{a + b - c}\right)^{-1}.$$

Dividing gives

$$(a, b, c) = \left(1 - \frac{1}{4}\left[a^2 + b^2 + c^2 - ab + ac + bc - \frac{3abc}{a + b - c}\right]\right)^{-1}.$$

So $\gamma > 0$ if and only if

$$\sup \frac{abc}{a + b - c} < \infty.$$

At this point, we must digress and recall some plane geometry from Ref. 12. First $abc/4$ is the area of the triangle and $2^{-1}(a + b + c)$ is called a semiperimeter. Given any triangle ABC, extend the two lines emanating from the apex A. Construct bisectors to the two exterior angles complementary to the angles B and C respectively. The bisectors meet in a point equidistant from the three lines containing a, b, and c. The circle tangent to these three lines is called an excircle. See Fig. 22. The center of the excircle (where the bisectors meet) is called the excenter and of course the radius is called the exradius. Each triangle has three excircles. Finally from Ref. 12 we need:

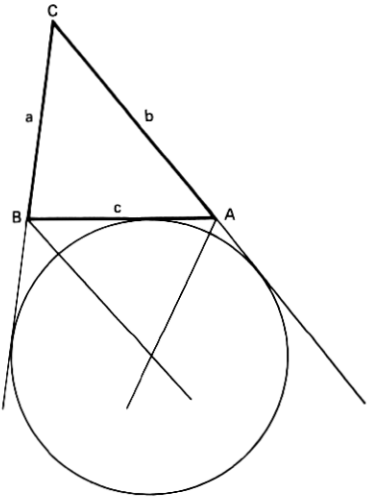

Fig. 22—Excircle tangent to c.

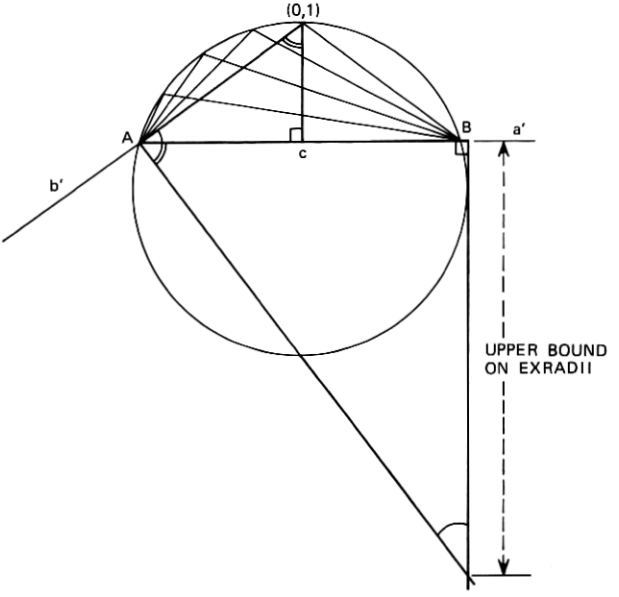

Fig. 23—Upper exradius bound for excircles tangent to c. Since $0 \leqq c \leqq 2$, the exradii are uniformly bounded.

Theorem: An exradius of a triangle is equal to the ratio of the area to the difference between the semiperimeter and the side to which the excircle is tangent internally.

So if the set of exradii of triangles circumscribed by the unit circle is uniformly bounded away from infinity, then $\gamma > 0$ and $\{\delta_\gamma\}_{0<\gamma<\gamma}$ are metrics.

To complete the proof, consider any triangle with vertices on the unit disc boundary. With an isometric transformation of the circle into itself, we can situate c horizontally with apex C above c in the left half-plane. The more obtuse the exterior angles at A and B, the larger the excircle tangent to c. So take a horizontal line a' through B and a line b' going through A and $(0, 1)$ and replace a and b with a' and b'. Clearly, bisectors constructed using a' and b' will intersect at a point further away from c than the excenter of any excircle tangent to c. By similar triangles, the primed bisectors intersect at a distance $2(1 \pm \sqrt{1 - c^2/4})$ from c where the sign is plus if c lies in the lower half-plane and negative otherwise (Fig. 23).

REFERENCES

1. Lucky, R. W., and Hancock, J. C., "On the Optimum Performance of N-ary Systems Having Two Degrees of Freedom," IEEE Trans. Commun. Syst. (March 1962).
2. Salz, J., Sheehan, J. R., and Paris, D. J., "Data Transmission by Combined AM and PM," B.S.T.J., *50*, No. 7 (September 1971), pp. 2399–2419.
3. Thomas, C. M., "Amplitude Phase-Keying with M-ary Alphabets: A Technique for Bandwidth Reduction," Int. Telemetering Conf. Proc., *VIII* (October 1972).
4. Gitlin, R. D., Ho, E. Y., and Mazo, J. E., "Passband Equalization of Differentially Phase-Modulated Data Signals," B.S.T.J., *52*, No. 2 (February 1973), pp. 129–238.
5. Viterbi, A. J., *Principles of Coherent Communication*, New York: McGraw-Hill, 1966, pp. 86–96 and 118–119.
6. Kernighan, B. W., and Lin, S., "Heuristic Solution of a Signal Design Optimization Problem," Proc. Seventh Annual Princeton Conf. on Information Sciences and Systems, March 1973.
7. Foschini, G. J., Gitlin, R. D., and Weinstein, S. B., "Optimization of Two-Dimensional Signal Constellations in the Presence of Gaussian Noise," to be published in IEEE Transactions on Communications.
8. Mazo, J. E., "A Note on Metrics and Metric Convexity," unpublished work.
9. Falconer, D. D., unpublished work.
10. Papoulis, A., *The Fourier Integral and Its Application*, New York: McGraw-Hill, 1962.
11. Jones, D. S. "Asymptotic Behavior of Integrals," SIAM Review, *14*, No. 2 (April 1972) pp. 286–317.
12. Davis, D. R., *Modern College Geometry*, Reading, Mass.: Addison-Wesley, 1957.